

NEW SMALL IMPACT CRATERS IN HIGH RESOLUTION HIRISE IMAGES - III. B. A. Ivanov¹, H. J. Melosh², A. S. McEwen², and the HiRISE team, ¹Institute for Dynamics of Geospheres, RAS, 119334, Moscow, Russia, baivanov@idg.chph.ras.ru, ²University of Arizona, Department of Planetary Sciences, Tucson, AZ, 85721.

Introduction: Repetitive imaging of Mars by various spacecraft revealed potential “new” impact sites [2, 3, 4, 5]: impact craters with documented time periods of formation, assuming that the appearances of dark spots correspond to crater formation. Impact crater clusters or crater strewn fields from primary impacts are found in MOC [1, 2], CTX, and HiRISE images [3, 4, 5] mostly in dusted areas. In 2009 the database for ~70 “new” craters has been processed. We present the new data analysis for small craters and crater clusters accumulated by the HiRISE team.

Size-frequency distribution: In the extended current database the formation of a single crater or one major crater observes in ~62% and prominent strewn fields are observed in ~38% cases. The single/multiple percentage depends on the effective size of cratering events (Fig.1). We find that clustered impacts (resulted from projectile’s atmospheric breakup) are equally or more frequent for largest “new” craters with effective diameters >20 m. Below this effective diameter single craters dominate in recorded impacts. In the most populated diameter bin $\langle D \rangle = 5.5$ m (3.9 m $\langle D_{eq} \rangle < 7.8$ m, 25 events totally), single craters are formed in 19 of 25 observed impact events. This observation allows us to update the discussion of the nature of multiply fragmented projectiles.

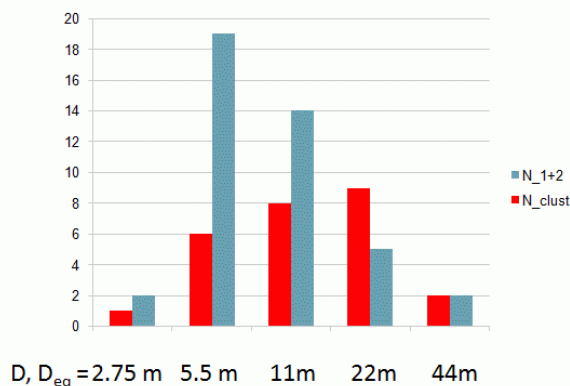


Fig. 1. Size-frequency distribution of single+major cratering impacts (gray) and clustered impacts vs. effective size of impacts. We measure diameters of all detected craters in each cluster and use the value of $D_{eff} = (\sum D_i^3)^{1/3}$ as an approximate measure of an effective crater that would be created by a non-dispersed projectile.

Halo and arcs around new craters: The systematic usage of CTX images to find new dark spots as well as the analysis of Themis, MOC, HRSC (and Viking – in one case) images improved our database. Many of newly formed (dated) impact sites have haloes as most of them are formed in dusty areas.

For ~70 fully processed impacts we can analyze properties of haloes – the important feature used to discover new impacts.

We measure (where available) the average size of dark halos around “new” craters. The whole data set on the ratio of the average halo width, D_H , to the crater diameter D , D_H/D , is shown in Fig. 2. Majority of impacts creates haloes with $D_H/D < 80$, while in extreme cases D_H/D ratio reaches 200 to 400.

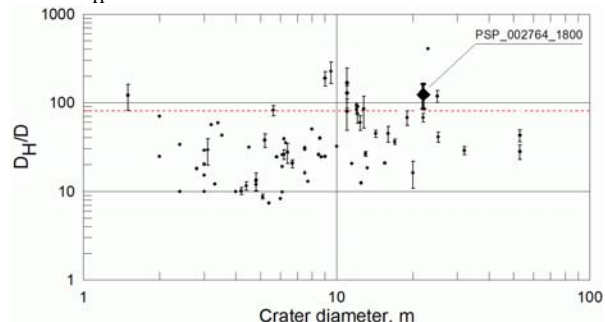


Fig.2. D_H/D for “new” impact craters vs. crater diameter (dots). PSP_002764_1800 case [6] is shown with a black diamond. Here the “dark halo” is formed by thousands of small dark streaks (“avalanches”) at dune slopes. The point just right of the black diamond is PSP_004030_1855 (Malin’s #13 [2]) impact site. Here the darkening around the impact site is smoother with only occasional “avalanches” at slopes.

Dark arcs (parabolas) around new craters: In 3 cases of multiple impacts we see dark arcs (“scimitars”, “parabolas”,) as relatively narrow curved strips extended well beyond the halo area (PSP_007496_1735 and 008045_2020, ESP_011618_1885). The width of these strips varies from 5 to 50 m for length of a few hundred meters.

In these three cases we find parabolic features (exemplified in Fig. 3) which may be treated as surface records of atmospheric shock wave interaction. To verify the idea the model of expanding hemispheric air shock waves is applied to find the theoretical curves of shock wave crossing. In all cases reasonably small (ms-range) assumed delay of smaller impacts vs. the

main impact results in a good fit to observed “parabolic” geometry (Fig. 4). It is important that in all cases smaller craters should be formed later than the main crater. This is in accord with the simple idea that smaller fragments of a projectile are stronger decelerated in the atmosphere after the breakup and reach surface a bit later. The direct modeling of atmospheric deceleration well fit the assumed time delay derived from the parabola geometry.

We should note that there is no visible influence of the ballistic wave of oblique impacts. In contrast in other three cases we find parabolic features of other kind without visible multiple craters (PSP_002764_1800=M07, PSP_003958_2095=M10, and PSP_004038_2005=M05; MXX is Malin’s catalogue numbers [2]).

The physical mechanism of enhanced dust removing along shock wave intersection lines may include both the interference of positive/negative pressure phases in crossing shock fronts and the atmospheric vortex origin behind the crossing line.

These observations constrain the surface structure of Martian surface in dusted areas. The presence of wide dark haloes and shock wave-related arcs witness in favor of thin (few mm) bright dust cover which may be relatively easy removed by transient events.

Conclusions: “New” impacts on observed by HiRISE effectively refresh the dusty surface in a style resembling the air shock wave interaction. Estimates show that at observed distances shock pressure in shock waves are of the order of a few or few tens of Pa. Nevertheless the shock wave crossing and reflection at the surface make clearly visible footprints. This phenomenon allows us to refine estimates of projectile density, velocity and impact angles using physics of atmospheric blast waves.

Acknowledgements: The work is supported by PGG contract # NNX08AM21G

References: [1] Popova O. P. et al. (2007) *Icarus* 190, 50-73. [2] Malin M.C. et al. (2006) *Science*, 314, 1573-1577. [3] Ivanov B.A., H.J. Melosh, and A.S. McEwen (2008) *LPS XXXIX*, Abstract #1402. [4] Ivanov B.A., H.J. Melosh, and A.S. McEwen (2008) *3d EPSC (Münster)*, Abstract # EPSC2008-A-00340. [5] Ivanov B.A., H.J. Melosh, and A.S. McEwen (2009) *LPS XXXX*, Abstract #1410. [6] Burleigh, K. J. Et al. (2009) *LPS XXXX*, Abstract #1431.

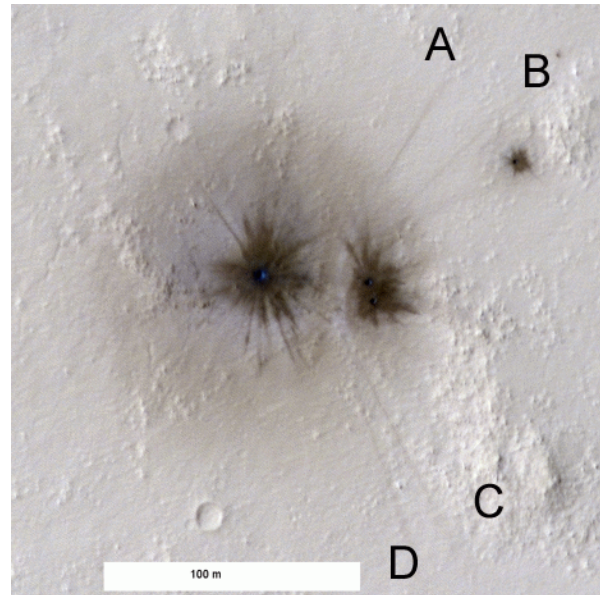


Fig. 3. PSP_008045_2020. Multiple impacts resulted from the projectile atmospheric breakup ($D_{eff}=5m$, totally 5 individual craters are visible). Parabolas A, B, C, and D extend ~ 100 m from the center. The most dark areas around individual craters are formed by ejecta deposition. Less contrasting wide haloes extend ~ 60 crater radii.

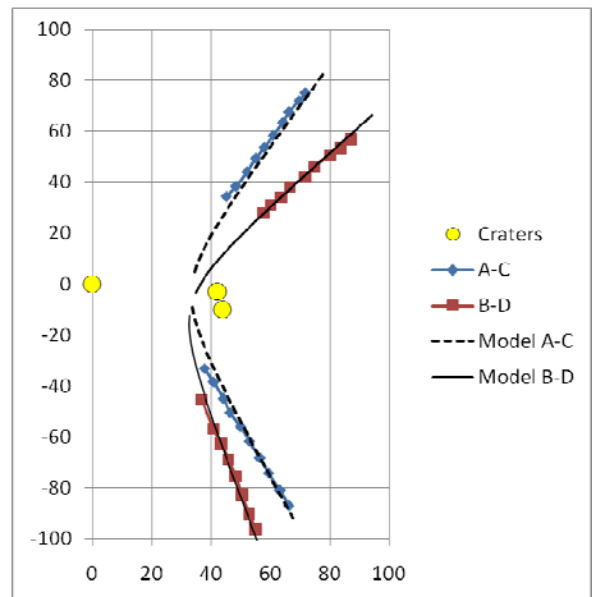


Fig. 3. PSP_008045_2020 (upper plate). Parabolas A, B, C, and D extend ~ 100 m from the center. The diagram (bottom plate) compares parabolas position and the model of shock front’s crossing assuming two smaller impacts delayed 96 and 103 ms after the major impact (distances on axis are in meters).